Long-range random transverse-field Ising model in three dimensions

István A. Kovács,[1,2,3,*] Róbert Juhász,[1,†] and Ferenc Iglói[1,2,‡]

[1]*Wigner Research Centre for Physics, Institute for Solid State Physics and Optics, H-1525 Budapest, P.O. Box 49, Hungary*

[2]*Institute of Theoretical Physics, Szeged University, H-6720 Szeged, Hungary*

[3]*Center for Complex Networks Research and Department of Physics, Northeastern University, 177 Huntington Avenue, Boston, Massachusetts 02115, USA*

(Received 28 January 2016; revised manuscript received 31 March 2016; published 31 May 2016)

We consider the random transverse-field Ising model in $d = 3$ dimensions with long-range ferromagnetic interactions which decay as a power $\alpha > d$ with the distance. Using a variant of the strong-disorder renormalization group method we study numerically the phase-transition point from the paramagnetic side. We find that the fixed point controlling the transition is of the strong-disorder type, and based on experience with other similar systems, we expect the results to be qualitatively correct, but probably not asymptotically exact. The distribution of the (sample dependent) pseudocritical points is found to scale with $1/\ln L$, L being the linear size of the sample. Similarly, the critical magnetization scales with $(\ln L)^{\chi}/L^{d}$ and the excitation energy behaves as $L^{-\alpha}$. Using extreme-value statistics we argue that extrapolating from the ferromagnetic side the magnetization approaches a finite limiting value and thus the transition is of mixed order.

DOI: 10.1103/PhysRevB.93.184203

I. INTRODUCTION

In nature there are magnetic materials in which ordering is due to long-range (LR) interactions which decay as a power $\alpha = d + \sigma$ with the distance. The best known examples are dipolar systems, such as the $LiHoF_4$. Putting this compound into an appropriate external magnetic field we obtain an experimental realization of a dipolar quantum ferromagnet [1]. Similar systems have been experimentally realized recently by ultracold atomic gases in optical lattices [2–6] and studied theoretically [7–17].

Concerning the phase-transitional properties of LR systems it has been known for quite some time that the universality class depends on the decay exponent, σ [18–22]. For a sufficiently large value of $\sigma > \sigma_U$ the transition is the same as in the short-range (SR) model, for intermediate values, $\sigma_L > \sigma > \sigma_U$, the critical behavior is nonuniversal and σ dependent, while for $\sigma < \sigma_L$ we have mean-field critical behavior. In low-dimensional systems LR forces could result in magnetic ordering and phase transitions, even if these are absent with SR interactions [23].

In the present paper we consider quantum magnets with LR interactions in the presence of quenched disorder. Such type of system is realized by the compound $LiHo_xY_{1-x}F_4$, in which a fraction of $(1 - x)$ of the magnetic Ho atoms is replaced by nonmagnetic Y atoms [1,24]. A related, but somewhat simplified [25] quantum model which describes the low-energy properties of this system is the random transverse-field Ising model with LR interactions given by the Hamiltonian:

$$\mathcal{H} = -\sum_{i \neq j} \frac{b_{ij}}{r_{ij}^{\alpha}} \sigma_i^x \sigma_j^x - \sum_i h_i \sigma_i^z. \tag{1}$$

Here, $\sigma_i^{x,z}$ are Pauli matrices, r_{ij} denotes the distance between site i and j, while the parameters b_{ij} and transverse fields h_i are independent identically distributed quenched random variables drawn from some distributions $p_0(b)$ and $g_0(h)$, respectively. In the following we restrict ourselves to ferromagnetic models, so that $b_{ij} > 0$ and $h_i > 0$.

We consider the system at zero temperature, when in the ground state there are two different phases: for strong (weak) enough transverse fields, $\overline{\ln h} > \tilde{\theta}$ ($\overline{\ln h} < \tilde{\theta}$), the system is in the paramagnetic (ferromagnetic) phase. (Here and in the following we use $\overline{\cdots}$ to denote averaging over quenched disorder.) The properties of phase transitions in random quantum Ising magnets with SR interactions are known to some extent [26–29], mainly due to strong-disorder renormalization group (SDRG) [30,31] studies. These results are then checked by numerical investigations in one [32,33] and two dimensions [34,35]. The main conclusion is that the critical behavior of SR random quantum Ising magnets at any finite dimension is governed by a so-called infinite-disorder fixed point (IDFP) [31,36], at which the dynamics is ultraslow: the length scale ξ and the time scale τ are related as follows: $\ln \tau \sim \xi^{\psi}$, where the exponent ψ is dimension dependent. This is in contrast with the scaling behavior at a conventional random fixed point: $\tau \sim \xi^z$, thus the dynamical exponent, z, is formally infinite at an IDFP.

The low-energy properties of the Hamiltonian in Eq. (1) in one dimension have already been studied through variants of the SDRG [37] (see also studies of the related hierarchical Dyson model [38] and that in Ref. [39]. In contrast to the SR case the critical behavior is found to be controlled by a strong-disorder fixed point, the critical dynamical exponent being finite: $z_c \simeq \alpha$. Qualitatively similar observations are found from the preliminary numerical SDRG results on the two-dimensional system in Ref. [40].

In this paper we extend these investigations to the experimentally more realistic three-dimensional system. Here we apply a numerical version of the SDRG method, which is expected to present physically correct results in the critical point approaching from the paramagnetic side. We find that the fixed point controlling the transition is of the strong-disorder type, and based on the experience with other similar systems,

*kovacs.istvan@wigner.mta.hu
†juhasz.robert@wigner.mta.hu
‡igloi.ferenc@wigner.mta.hu

we expect the results to be qualitatively correct, but probably not asymptotically exact. We study in detail the distribution of the sample-dependent critical points, the scaling behavior of the magnetization, and that of the low-energy excitations. The SDRG results are then interpreted in the frame of extreme-value statistics (EVS) [41], which is then used to make conjectures about the scaling behavior of the different quantities at the ferromagnetic side of the transition point. Most surprisingly the average magnetization is expected to approach a finite limiting value, thus the transition is of mixed order.

The rest of the paper is organized as follows. In Sec. II we recapitulate the basic features of the SDRG method and discuss its particular form for LR systems. In Sec. III we present our results of the numerical SDRG analysis, which is then interpreted within the frame of EVS in Sec. IV. Our results are discussed in Sec. V.

II. SDRG METHOD FOR LR INTERACTIONS

In the SDRG method the decimation procedure is performed locally in real space according to the value of the excitation energy. At each step of the renormalization the largest local parameter of the Hamiltonian is eliminated and between the remaining degrees of freedom new, renormalized parameters are calculated perturbatively. Let us consider a general graph with vertices denoted by $i,j,k,l,\ldots$. After decimating the strongest coupling, J_{ij}, (in our case $J_{ij}=\frac{b_{ij}}{r_{ij}^{\alpha}}$) the two sites i and j form a cluster of spins in an effective transverse field: $\tilde{h}=h_i h_j/J_{ij}$. On the contrary, if the strongest transverse field, h_i, is decimated, then between sites, j and k—which are originally nearest neighbors to i—a new coupling is created: $\tilde{J}_{jk}=\max(J_{jk},J_{ji}J_{ki}/h_i)$. Here in the last step the so-called maximum rule is applied, which is essential in the fast algorithm [29] we use in the numerical calculation. In the starting steps of the decimation the maximum rule can be a crude approximation; however, it becomes more and more correct by approaching the fixed-point distributions. Generally we can say that the use of the maximum rule is correct in the paramagnetic phase and asymptotically correct at an IDFP. If the fixed point under consideration is just a strong-disorder one, then the maximum rule is a good approximation, which generally does not modify the qualitative behavior of the model. We note, however, that the maximum rule is certainly not correct in the ferromagnetic phase, in particular for LR models.

In the numerical application of the SDRG method we start with some initial disorder; in our case we have used box distributions: the parameters of the model were chosen uniformly from the intervals $b_{ij}\in(0,1]$ and $h_i\in(0,h]$, so that the control parameter is defined as $\theta=\ln(h)$. Now let us assume for a moment that our model is short ranged, i.e., in Eq. (1) $\frac{b_{ij}}{r_{ij}^{\alpha}}$ is replaced with b_{ij} and the first sum runs over nearest neighbors. At the critical point of the SR model ($\theta_c^{\rm SR}$) the decimation procedure is asymptotically symmetric in one dimension (1D): couplings and transverse fields are decimated with the same fraction. The resulting cluster structure is illustrated in Fig. 1. In higher dimensions the ratio of the frequency of coupling and transverse-field decimations has a finite limiting value, $r_{\rm SR}=O(1)$. Now switching on the LR forces, the renormalization procedure starting from $\theta_c^{\rm SR}$ will turn to be more and more asymmetric due to the appearance of new LR couplings: below some energy scale almost always couplings will be decimated and the LR model renormalizes to the ferromagnetic fixed point. Consequently the critical point of the LR model satisfies the relation $\theta_c>\theta_c^{\rm SR}$.

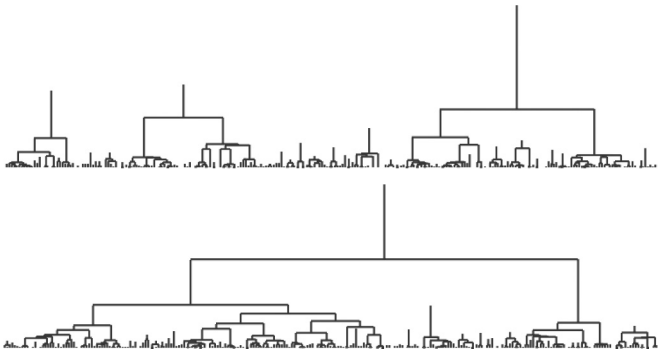

FIG. 1. Illustration of the spin clusters formed during the SDRG process at the critical point of the 1D short-range random transverse-field Ising model for two samples at $L=256$. The fate of a spin cluster is either to be decimated out (indicated by vertical spikes) or to be fused together with an other spin cluster (horizontal lines). Higher trees indicate clusters being present at later stages of the SDRG procedure, corresponding to the low-energy modes of the system. The magnetic moment is related to the size of the largest cluster, scaling as $\mu(L)\propto L^{d_f}$, where the fractal dimension is $d_f=\frac{\sqrt{5}+1}{4}\approx 0.809$ [26].

Now let us follow the renormalization procedure of the LR model starting from its own critical point θ_c, when three different regimes can be identified. At the *initial period* predominantly nearest-neighbor couplings are involved and the renormalization proceeds basically as in the SR model. Since at θ_c the SR model is in the paramagnetic phase in the initial period almost exclusively, transverse fields are decimated and the distribution of the renormalized transverse fields will approach the known form [31]:

$$g(h)=\frac{d}{z}h^{-1+d/z}, \tag{2}$$

with some effective dynamical exponent, $z\approx z^{\rm SR}(\theta_c)$ of the SR model at the control parameter θ_c. The initial period of the RG ends when the generated new couplings become in the same order as the existing LR bonds. In the following *intermediate period* predominantly transverse fields are decimated, but among the renormalized couplings—due to the maximum rule—there are more and more original LR bonds. As a result the distribution of the transverse fields will continuously change, and the value of the effective dynamical exponent increases further and approaches its asymptotic value at the critical point, z_c. In the final, *asymptotic regime* in the decimation mainly transverse fields are involved, but also a fraction, r, of LR couplings are decimated, too. (As the critical fixed point is approached r tends to zero; the calculated scale dependence is shown in Sec. III.) The generated new couplings are almost always smaller than the existing LR bonds, thus according to the maximum rule these original couplings play

TABLE I. Properties of the critical SDRG procedure in the different regimes (see text).

RG period	Decimation	Couplings	$z_{\rm eff}$
Initial	h	SR	$\approx z^{\rm SR}(\theta_c)$
Intermediate	h	SR and LR	$z^{\rm SR}(\theta_c) < z_{\rm eff} < z_c$
Asymptotic	h and J	LR	z_c

the role of the renormalized ones. Consequently at the fixed point the decimation of a transverse-field results in the erasure of the given site together with the couplings starting from it. The basic ingredients of the RG procedure in the three regimes are summarized in Table I. The final cluster structure of the LR model in 1D is illustrated in Fig. 2: comparing to the SR model here the clusters have smaller extent and contain less sites. In higher dimensions, in two dimensions (2D) and three dimensions (3D) we show in Fig. 3 the structure of the largest clusters, in which the critical properties of the model are encoded. Even in higher dimensions these clusters are sparse and they can be embedded in a quasi-one-dimensional object. This last property is shared with the largest critical clusters in SR models.

III. NUMERICAL SDRG ANALYSIS

Here we present our numerical results for the three-dimensional LR model, which are obtained by the use of the fast SDRG algorithm in Ref. [29]. In the calculations we used finite samples with periodic boundary conditions of linear size up to $L = 24$ and the LR interaction is truncated at maximum distance $r \sim L$. The number of samples was typically 100 000 (at least 2000 for the largest size) and the box distributions are used, as described before. We have fixed the decay exponent to $\alpha = 4$ and calculated sample-dependent pseudocritical points, as described in Ref. [28]. In this method we consider two copies of the same sample, say $\mathcal{A}$. To be specific, we start with a sample and at an arbitrary position cut the interactions in each of the three directions with a plane and insert an equivalent copy into the gap while reconnecting the cut links. We note, that the obtained replicated sample is unique and does not depend on the chosen gap positions. On this replicated system we perform the decimation procedure until the last effective cluster. In the ferromagnetic (paramagnetic) phase the renormalization histories in the two copies are correlated (uncorrelated) and the boundary value of the parameter, $\theta_c(\mathcal{A})$, defines the pseudocritical point of the given sample. The distribution of the pseudocritical points is shown in Fig. 4: both the position of the maximum and the width of the distribution follows a $1/\ln L$ scaling, from which the true critical point is estimated at $\theta_c = 3.25(15)$. The scaling behavior of the distribution of the pseudocritical points is compatible with an exponential increase of the correlation length, at least from the paramagnetic side:

$$\xi \sim \exp\left[\text{const}/(\theta - \theta_c)\right], \qquad \theta > \theta_c. \tag{3}$$

At the critical point we calculated the fraction of decimation steps which involves a coupling and that which involves a transverse field. Their ratio, $r_{\theta_c}(L)$, is given by the ratio of the accumulated distributions of the pseudocritical points on the two sides of θ_c. We obtained a logarithmic L dependence: $r_{\theta_c}(L) \sim 1/(\ln L)^{\omega}$, with $\omega \approx 2$, as in the 1D case as illustrated in Fig. 5.

At the critical point, we have also calculated the average mass of the last remaining cluster $\mu(L) = L^d m(L)$, $m(L)$ being the local magnetization and the characteristic time scale $\tau(L)$ defined as $\tau = 1/\tilde{h}$, where $\tilde{h}$ is the last decimated parameter in a finite sample.

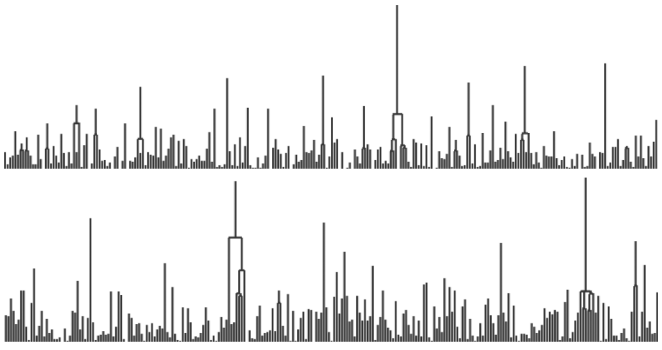

FIG. 2. The same dendrogram illustration as in Fig. 1 for the critical 1D long-range random transverse-field Ising model at $L = 256$. As opposed to the short-range model, mostly transverse fields are decimated resulting in spikes and smaller spin clusters, following a scaling of the form $\mu(L) \propto \ln^2 L$.

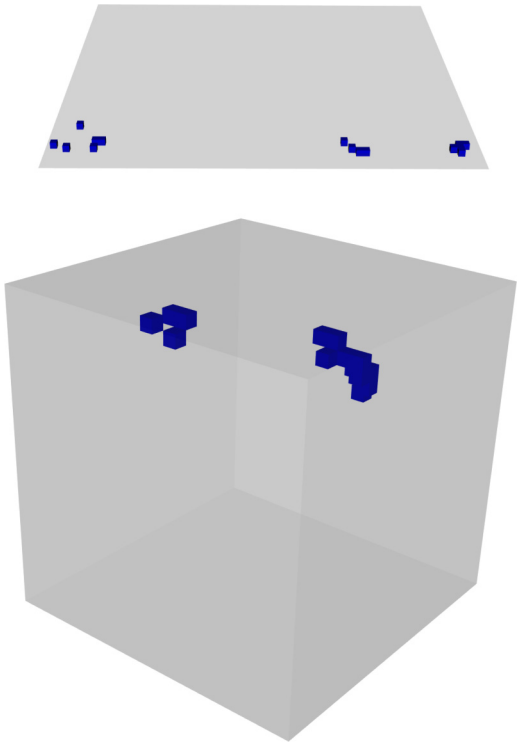

FIG. 3. The large-scale spin clusters of the critical long-range random transverse-field Ising model appear to be sparse and they can be embedded in a quasi-one-dimensional object, as illustrated in 2D ($L = 64$) and 3D ($L = 24$). The size of these clusters provides the magnetic moment following a similar scaling as in 1D as shown in Eq. (4).

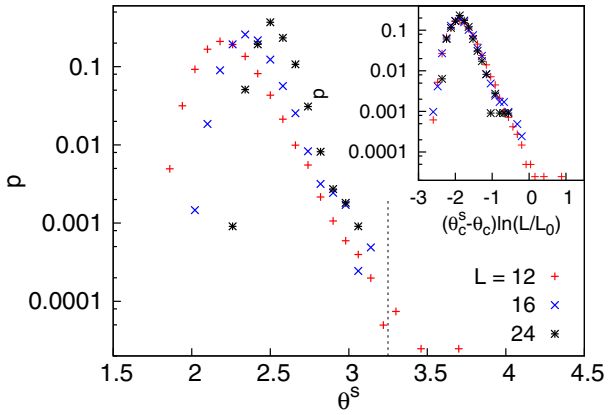

FIG. 4. Distribution of the pseudocritical points, which are estimated to cross each other for different L at $\theta_c \approx 3.25$, is indicated by a dotted line. The ratio of the accumulated distributions on two sides of θ_c is given by $r_{\theta_c}(L)$ (see the text and Fig. 5). The inset shows the rescaled distributions with $L_0 = 2$.

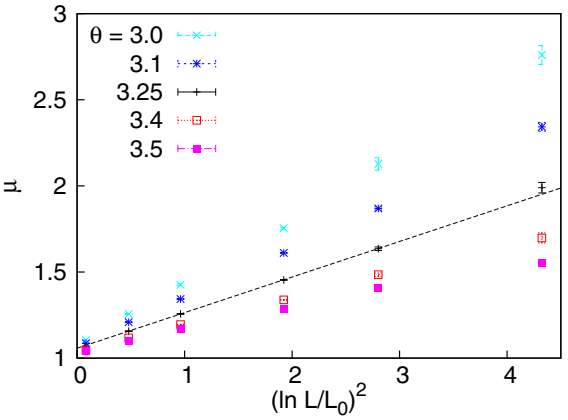

FIG. 6. The average mass of the last decimated cluster plotted against $(\ln L/L_0)^2$ with $L_0 = 3.2$. The data has been obtained by numerical renormalization of the three-dimensional model with decay exponent $\alpha = 4$, for different values of the control parameter θ.

The numerical results indicate that the magnetic moment $\mu(L)$ has a slower-than-algebraic dependence, which can be written in analogy with the one-dimensional result as

$$\mu(L) \sim [\ln(L/L_0)]^{\chi}. \tag{4}$$

Precise determination of χ from the existing numerical results is difficult, since it is sensitive to the value of the reference length, L_0. The data in Fig. 6 are compatible with $\chi = 2$ with $L_0 = 3.2$, but a similar fit is obtained with $\chi = 3$ if we choose $L_0 = 2$ instead.

Calculating the average logarithmic time scale, $\overline{\ln \tilde{h}}$, estimates of an effective, size-dependent dynamical exponent, $z(L)$, has been obtained from two-point fits of the relation

$$\overline{\ln \tilde{h}} = -z \ln L + \text{const.} \tag{5}$$

The extrapolation of $z(L)$ to infinite system size is shown in Fig. 7. At the critical value of $\theta = 3.25$ the data points seem to have a $1/\ln L$ correction and the extrapolated value is compatible with the expectation $z_c = \alpha = 4$.

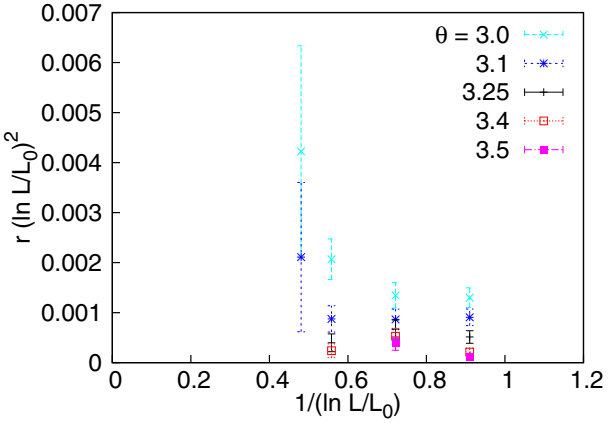

FIG. 5. The scaled decimation ratio, $r_{\theta_c}(L)$, as a function of the L size at $L_0 = 2$, indicating a similar logarithmic scaling as in 1D.

The dynamical exponent—according to Eq. (2)—is involved in the distribution of the last decimated transverse fields [see Eq. (6)], which is illustrated in Fig. 8. At the critical point [see in Fig. 8(a)], the numerical value of the critical dynamical exponent is compatible with $z_c = \alpha$. In the paramagnetic phase the distribution of the last decimated transverse fields is still in agreement with Eq. (2), but the dynamical exponent is $z < z_c$ [see in Fig. 8(b)].

We close this section by presenting the SDRG phase diagram of the LR random transverse-field Ising model obtained with the maximum rule (see in Fig. 9). Here we use the parameters α/z [z is an effective exponent, which appears in the distributions of the transverse fields in Eq. (2); see also in Table I] and r (the ratio of the decimation frequencies of the couplings and the transverse fields). According to our numerical calculations the phase diagram has the same qualitative features in one [37] and two dimensions [40], too. (In one dimension the phase diagram is related to that of random Josephson junctions [42]). As seen in Fig. 9

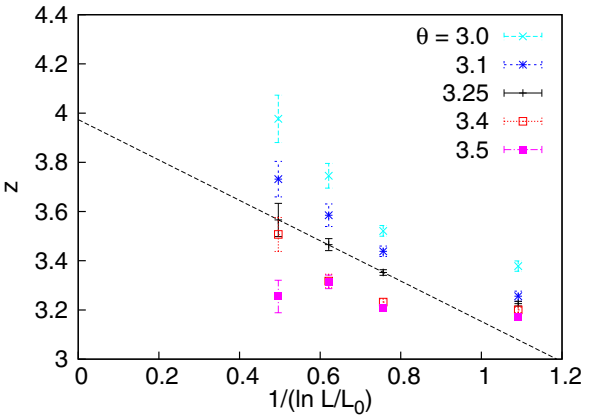

FIG. 7. Effective dynamical exponents obtained by two-point fits using Eq. (5) as a function of the system size L. The straight line, which connects the data obtained for the critical value $\theta = 3.25$ is a guide to the eye.

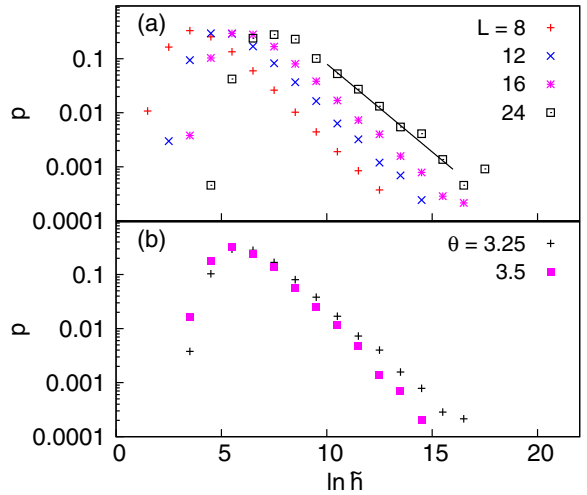

FIG. 8. (a) Distributions of the last decimated transverse fields at the critical point for different sizes. The straight line indicates the asymptotic shape of the tail according to EVS, with $z = \alpha$ (see text). (b) As the dynamical exponent, z decreases, the shape of the distribution changes in the paramagnetic phase as illustrated at $L = 16$.

there is a line of fixed points at $r = 0$, at which almost exclusively transverse fields are decimated. For $\alpha/z > 1$ these fixed points are stable and control the paramagnetic phase and the corresponding Griffiths singularities [43], while for $\alpha/z < 1$ the fixed points are unstable and the RG flow scales to $r \to \infty$, which corresponds to the ferromagnetic phase. In this regime the maximum rule in the SDRG procedure is certainly not valid. The two regimes of fixed points are separated by the critical fixed point at $\alpha/z = 1$. In the following section we

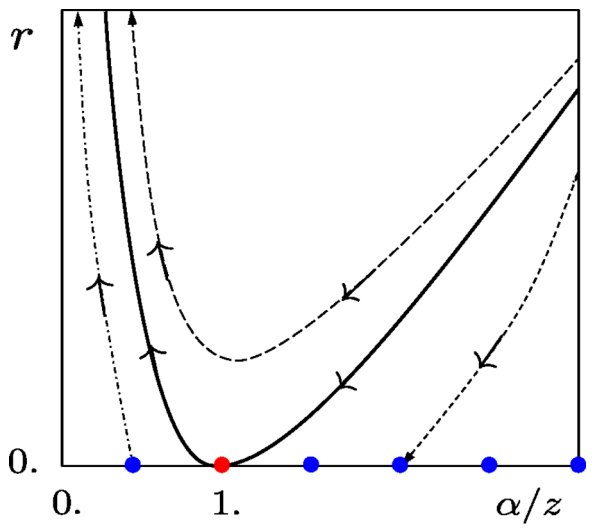

FIG. 9. Schematic SDRG phase diagram obtained through the maximum rule: the arrows indicate the direction the parameters evolve as the energy scale is reduced. Fixed points (blue circles) are at $r = 0$: the attractive fixed points of the paramagnetic phase ($\alpha/z > 1$) and the repulsive ones ($\alpha/z < 1$) are separated by the critical fixed point (red circle); see the text.

analyze the scaling behavior of the system in the vicinity of $r = 0$ and $\alpha/z = 1$ through extreme value statistics.

IV. ANALYSIS OF THE CRITICAL BEHAVIOR TROUGH EVS

A. Critical point

At the critical point in the asymptotic regime of the RG mainly transverse fields are decimated, but occasionally LR bonds are decimated, too. Let us consider a finite system of linear length, L, and concentrate on the largest cluster, which contains $\mu + 1$ sites. In this cluster altogether μ LR bonds *have been decimated*, and let us denote them by $J_i = b_i r_i^{-\alpha}$ where $i = 1,2,\ldots,\mu$ is the order of decimation. In this cluster the transverse fields h_i, $i = 1,2,\ldots,\mu+1$, *are not decimated* out, thus $J_i \gtrsim h_i$, J_i being the only decimated coupling in a region of linear size r_i, while h_i is the smallest one out of $\sim r_i^d$ transverse fields. Since the transverse fields in the asymptotic regime have a power-law distribution, see that in Eq. (2) the h_i is given by EVS as $h_i \simeq \kappa_i r_i^{-z}$ where κ_i are random numbers which are distributed according to the Fréchet statistics:

$$P(\kappa) = \frac{d}{z}\kappa^{d/z-1}\exp(-\kappa^{d/z}). \tag{6}$$

The effective transverse field of the cluster is given by $\tilde{h} \sim \prod_{i=1}^{\mu+1} h_i / \prod_{i=1}^{\mu} J_i \sim h_{\mu+1}\prod_{i=1}^{\mu}(r_i^{\alpha-z}\kappa_i/b_i)$. This scales differently for $\overline{\ln(J)} > \overline{\ln(h)}$ and for $\overline{\ln(J)} < \overline{\ln(h)}$, where the overbar denotes averaging over disorder. Thus at the critical point $\alpha = z_c$ and $\overline{\ln(b)} = \overline{\ln(\kappa)}$. This result about the dynamical exponent at the critical point agrees with our numerical results in the previous section. For the given cluster at the critical point the effective transverse field is given by $\tilde{h} \sim \prod_{i=1}^{\mu}(\kappa_i/b_i)$ (since $h_{\mu+1} = \mathcal{O}(1)$). If κ_i and b_i are not (or just weakly) correlated, then according to the central limit theorem $\ln\tilde{h} \sim \mu^{1/2}$. More generally we can write $\ln\tilde{h} \sim \mu^{1/\chi}$, what is to be compared with $\ln\tilde{h} \sim -\alpha \ln L$, which implies $\mu \sim (\ln L)^{\chi}$, in agreement with Eq. (4).

B. Paramagnetic side

In the paramagnetic phase, $\theta > \theta_c$, the distribution of the transverse fields in Eq. (2) involves the dynamical exponent $z < \alpha$ and in the vicinity of the transition points $\alpha - z = \delta\alpha/d$ and $\delta \sim \theta/\theta_c - 1 \ll 1$. Here the correlation length, $\xi(\delta)$, is defined by the length of the longest decimated bond, r_l, the corresponding coupling $J_l = b_l r_l^{-\alpha}$ being larger than the smallest transverse field, $h_l \simeq \kappa_l r_l^{-\alpha(1-\delta/d)}$. Consequently $\kappa_l < \xi^{-\delta\alpha/d}$ or $\mathrm{Prob}(\kappa_l < \xi^{-\delta\alpha/d}) = O(1)$, which can be written using Eq. (6) as

$$\int_0^{\xi^{-\delta\alpha/d}} P(\kappa)d\kappa = 1 - \exp(-\xi^{-\delta}) \approx \xi^{-\delta} = O(1), \tag{7}$$

for $z \approx \alpha$. Consequently in the paramagnetic phase the correlation length is given by $\ln\xi \sim 1/\delta$, in agreement with Eq. (3).

The dynamical behavior of the system in the paramagnetic phase is governed by Griffiths singularities, which are due to rare regions, in which the system is locally in its ferromagnetic phase. Here we recapitulate the so-called optimal fluctuation

argument [44] for the SR model and then generalize it to the LR case. The probability, $P(\ell)$, to find an ordered domain of linear size ℓ in the paramagnetic phase is exponentially small: $\ln P(\ell) \sim (\ell/\xi)^d$, but its excitation energy, $\epsilon_{\rm SR}(\ell)$—estimated through an ℓ^d-order perturbation theory in h_i/J_{ij}—is also exponentially small: $\ln \epsilon_{\rm SR}(\ell) \sim (\ell/l_0)^d$. Combining these two effects a power-law distribution of $\epsilon_{\rm SR}$ is observed, with a dynamical exponent $z_{\rm SR} = d(\xi/l_0)^d$. In the LR model we first assume that the rare regions are localized, too, then the form of $P(\ell)$ remains the same; however, by estimating the excitation energy one should take into account the LR forces, too. Let us assume that the ordered cluster of linear size ℓ is the largest one (and thus has the smallest excitation energy) within a region of linear size L, where $L^d P(\ell) = O(1)$, thus $\ln L \approx \frac{1}{d}(\ell/\xi)^d$. Within this controlled region the distance between the largest and the second largest cluster is $\sim L$ and the direct LR interaction between them is $\epsilon_{\rm LR} \sim L^{-\alpha}$. Now in the LR model the actual value of the excitation energy in the controlled domain is obtained by comparing the SR and LR contributions and is given by $\epsilon(\ell) = \max[\epsilon_{\rm SR}(\ell),\epsilon_{\rm LR}(L)]$, or $\ln \epsilon(\ell) = \max[-(\ell/l_0)^d, -\alpha/d(\ell/\xi)^d]$. This means that the effective volume scale in the SR model, l_0^d, is replaced by $\max[\frac{d}{\alpha}\xi^d, l_0^d]$ in the LR model. Consequently the dynamical exponent in the LR model is given by $z = \min[z_{\rm SR},\alpha]$, i.e., it is bounded by $z = z_c = \alpha$, which is the value at the critical point, as observed numerically. Our numerical results in Sec. III are in favor of our assumption that the rare regions in the LR models are localized, too.

C. Ferromagnetic side

In the ferromagnetic phase, $\theta < \theta_c$, we analyze the SDRG solution with the maximum rule, starting from the unstable fixed points in the vicinity of the critical fixed point (see in Fig. 9). We expect that the asymptotic results in the vicinity of the transition point do not depend on the actual direction—how the transition point is approached from the ferromagnetic phase. In these fixed points the distribution of the transverse fields is given in Eq. (2) with $z = \alpha(1 + \delta/d)$ and $\delta \sim 1 - \theta/\theta_c \ll 1$. In the ferromagnetic phase there is a giant connected cluster and the length scale, ξ, is defined by the linear extent of the largest hole in it. This is defined by the length of the longest decimated bond, r_l, so that all the transverse fields are decimated out within this region. The strength of this bond now satisfies $J_l/h_l \sim r_l^{\delta\alpha/d}/\kappa_l < 1$. This means, that $\mathrm{Prob}(\kappa_l > \xi^{\delta\alpha/d}) = \mathcal{P} = O(1)$ and here we assume once more, that $P(\kappa)$ can be described by the Fréchet distribution:

$$\int_{\xi^{\delta\alpha/d}}^{\infty} P(\kappa)d\kappa = \exp(-\xi^{\delta}) = \exp(-e^{-C}) = \mathcal{P}, \qquad (8)$$

thus $\xi \sim \exp(-C/\delta)$. Evidently ξ has different scaling behavior for $C < 0$ ($0 < \mathcal{P} < 1/e$) and for $C > 0$ ($1/e < \mathcal{P} < 1$). In the former case ξ is divergent for $\delta \to 0$ as in the paramagnetic side, but for $C > 0$ the correlation length in the continuum description goes to zero and the magnetization is of $O(1)$ for $\delta \to 0$. Here—depending on the possible set of values of $\mathcal{P}$ in the different samples—we can have two different scenarios concerning the behavior of the average magnetization at the transition point.

1. Second-order transition

If, for some reason, $\mathcal{P}$ is smaller than $1/e$ in every sample, then we always have $C < 0$ and the average magnetization vanishes at $\delta \to 0$, thus the phase transition is of second order. In this case the average correlation length diverges exponentially, as in the paramagnetic side.

2. Mixed-order transition

If, however, $\mathcal{P}$ is not bounded by $1/e$ and there is a finite fraction of the samples with $1/e < \mathcal{P} < 1$, thus $C > 0$, then the average magnetization goes to a finite limiting value as the transition point is approached from the ferromagnetic side. At the same time the average correlation length is exponentially divergent, thus the transition is of mixed order.

At the moment we have no information about the possible values of $\mathcal{P}$, and with the lack of any known constraints we are inclined to prefer the mixed-order transition scenario. It is in the spirit of Occam's razor, since in this case we have to use fewer assumptions. Mixed-order transitions often appear in pure systems with LR forces [45–51]; our model then would represent such a phenomena in the presence of random LR interactions.

V. DISCUSSION

In this paper we have studied the critical properties of the random transverse-field Ising model in 3D with the presence of LR forces. Our present work completes our investigations starting in 1D [37] and continued in 2D by announcing some numerical results [40]. This problem is technically quite difficult and the only possible method of numerical investigations at present seems to be the SDRG approach. Here we used a variant of it based on the so-called maximum rule, which enabled us to study sufficiently large systems (up to linear size $L = 24$) with an appropriate statistics.

Here we should note that although the Hamiltonian is fully connected, as the coupling strength decays fast enough (the total interaction energy is extensive) one expects that it is still sensible to speak about a local order parameter and to identify ferromagnetic and paramagnetic domains by an SDRG procedure as for the short-range model. Applying the SDRG scheme based on the maximum rule in the paramagnetic phase or in the critical point leads to—the cluster formations being rare—a sparse distribution of ferromagnetic clusters, which makes the SDRG procedure at least internally consistent. This is due to the fact that by decreasing the energy scale, an overwhelming fraction of the original spins are eliminated as being locally paramagnetic and not playing a role in the low-energy physics. For such a sparse distribution of ferromagnetic domains, which are themselves sparse sets of original spins, it is a reasonable approximation to keep as an effective coupling between clusters only the strongest LR coupling, which is typically the coupling between the closest spins. This is essentially nothing but the maximum rule. In one dimension, we went beyond the maximum rule by taking into account the sum of LR couplings between all pairs of spins of adjacent cluster (see Refs. [37,40]), but this did not lead to changes in the results in leading order, so this approximation (i.e., maximum rule instead of sum rule) is quite good. Also

the vanishing of the relative frequency of bond decimations persists in this improved scheme, so it is not an artifact of the simplified maximum rule. Thus, assuming that disorder plays a relevant role in determining low-energy properties, our SDRG method must be a reasonable approximation. We have checked the consequences of the strong-disorder scenario for the LR contact process by Monte Carlo simulations in Ref. [40] and found agreement for not too small values of α. This justifies indirectly the applicability of the SDRG method.

The obtained RG phase diagram in Fig. 9 has the same qualitative structure as that in lower dimensions: both the phase-transition point and the fixed points controlling the paramagnetic phase with Griffiths singularities are located at $r = 0$ and are characterized by parameter-dependent dynamical exponents. In these attractive fixed points almost exclusively transverse fields are decimated and the renormalized couplings, according to the maximum rule, are selected from the original LR bonds and their value can be estimated from EVS. We have found that the average correlation length at the transition point diverges exponentially [see Eq. (3)], but the average magnetization—in the spirit of Sec. IV C 2—is expected to have a finite jump at the transition point. Therefore we conjecture that the transition is of mixed order. Mixed-order transitions have already been observed in different systems: in the classical LR Ising chain with $\alpha = 2$ [45–51], in models of depinning transition [52–55], and in percolation models with glass and jamming transition [56–65] (for a recent review see Ref. [66]). Our study indicates that such a phenomenon could take place also in disordered quantum systems with LR forces.

At the transition point the magnetization in a finite sample scales logarithmically [see Eq. (4)] and the dynamical exponent is finite, $z_c = \alpha$, thus the critical fixed point is a strong-disorder fixed point, but not an infinite-disorder one. In this case our analysis does not guarantee that the obtained SDRG results are asymptotically exact: to prove this one should have performed a second-order treatment of the perturbation calculation. However, based on our experience with other systems having a strong-disorder fixed point [67], we expect that our SDRG results are very probably qualitatively correct and also the numerical estimates are reliable. Considering the application of the maximum rule in our numerical algorithm it has a negligible effect in the paramagnetic phase, in which the typical size of ferromagnetic clusters is finite. At the transition point we expect to have at most logarithmic corrections to the results obtained by the maximum rule. Finally, at the ferromagnetic phase the maximum rule does not hold any longer, but the predicted jump of the magnetization at the transition point most probably remains true together with the mixed-order nature of the transition.

Our results are expected to hold for a large class of disordered LR quantum models having a discrete symmetry, such as the random quantum Potts and Ashkin-Teller models [31]. The critical fixed point of the model in Eq. (1) is expected to govern the critical behavior of some random stochastic models, such as the random contact process, at least for strong enough disorder. For SR forces this type of mapping has been known for quite some time [68,69], and its validity has also been demonstrated with LR interactions in 1D and 2D [40,70].

ACKNOWLEDGMENT

This work was supported by the Hungarian Scientific Research Fund under Grant No. K109577.

[1] For a review, see A. Dutta, G. Aeppli, B. K. Chakrabarti, U. Divakaran, T. F. Rosenbaum, and D. Sen, *Quantum Phase Transitions in Transverse Field Spin Models: From Statistical Physics to Quantum Information* (Cambridge University Press, Cambridge, 2015).
[2] A. Friedenauer, H. Schmitz, J. T. Glueckert, D. Porras, and T. Schaetz, Nat. Phys. **4**, 757 (2008).
[3] K. Kim, M.-S. Chang, S. Korenblit, R. Islam, E. E. Edwards, J. K. Freericks, G.-D. Lin, L.-M. Duan, and C. Monroe, Nature (London) **465**, 590 (2010).
[4] R. Islam, E. E. Edwards, K. Kim, S. Korenblit, C. Noh, H. Carmichael, G.-D. Lin, L.-M. Duan, C.-C. J. Wang, J. Freericks, and C. Monroe, Nat. Commun. **2**, 377 (2011).
[5] J. W. Britton, B. C. Sawyer, A. C. Keith, C. J. Wang, J. K. Freericks, H. Uys, M. J. Biercuk, and J. J. Bollinger, Nature (London) **484**, 489 (2012).
[6] R. Islam, C. Senko, W. C. Campbell, S. Korenblit, J. Smith, A. Lee, E. E. Edwards, C.-C. J. Wang, J. K. Freericks, and C. Monroe, Science **340**, 583 (2013).
[7] D. Porras and J. I. Cirac, Phys. Rev. Lett. **92**, 207901 (2004).
[8] X. L. Deng, D. Porras, and J. I. Cirac, Phys. Rev. A **72**, 063407 (2005).
[9] P. Hauke, F. M. Cucchietti, A. Müller-Hermes, M. Bañuls, J. I. Cirac, and M. Lewenstein, New J. Phys. **12**, 113037 (2010).
[10] D. Peter, S. Müller, S. Wessel, and H. P. Büchler, Phys. Rev. Lett. **109**, 025303 (2012).
[11] V. Nebendahl and W. Dür, Phys. Rev. B **87**, 075413 (2013).
[12] M. L. Wall and L. D. Carr, New J. Phys. **14**, 125015 (2012).
[13] S. A. Cannas and F. A. Tamarit, Phys. Rev. B **54**, R12661(R) (1996).
[14] A. Dutta and J. K. Bhattacharjee, Phys. Rev. B **64**, 184106 (2001).
[15] M. Dalmonte, G. Pupillo, and P. Zoller, Phys. Rev. Lett. **105**, 140401 (2010).
[16] T. Koffel, M. Lewenstein, and L. Tagliacozzo, Phys. Rev. Lett. **109**, 267203 (2012).
[17] P. Hauke and L. Tagliacozzo, Phys. Rev. Lett. **111**, 207202 (2013).
[18] M. E. Fisher, S. K. Ma, and B. G. Nickel, Phys. Rev. Lett. **29**, 917 (1972).
[19] J. Sak, Phys. Rev. B **8**, 281 (1973).
[20] E. Luijten and H. W. J. Blöte, Phys. Rev. Lett. **89**, 025703 (2002).
[21] M. Picco, arXiv:1207.1018; T. Blanchard, M. Picco, and M. A. Rajabpour, Europhys. Lett. **101**, 56003 (2013).

[22] M. C. Angelini, G. Parisi, and F. Ricci-Tersenghi, Phys. Rev. E **89**, 062120 (2014).

[23] F. J. Dyson, Commun. Math. Phys. **12**, 91 (1969); **12**, 212 (1969).

[24] D. H. Reich, B. Ellman, J. Yang, T. F. Rosenbaum, G. Aeppli, and D. P. Belanger, Phys. Rev. B **42**, 4631 (1990); W. Wu, B. Ellman, T. F. Rosenbaum, G. Aeppli, and D. H. Reich, Phys. Rev. Lett. **67**, 2076 (1991); W. Wu, D. Bitko, T. F. Rosenbaum, and G. Aeppli, *ibid.* **71**, 1919 (1993); J. Brooke, D. Bitko, T. F. Rosenbaum, and G. Aeppli, Science **284**, 779 (1999).

[25] In this compound the transverse field also induces a random longitudinal field via the off-diagonal terms of the dipolar interaction. See in S. M. A. Tabei, M. J. P. Gingras, Y. J. Kao, P. Stasiak, and J. Y. Fortin, Phys. Rev. Lett. **97**, 237203 (2006); M. Schechter, Phys. Rev. B **77**, 020401(R) (2008); M. Schechter and P. C. E. Stamp, Europhys. Lett. **88**, 66002 (2009).

[26] D. S. Fisher, Phys. Rev. Lett. **69**, 534 (1992); Phys. Rev. B **51**, 6411 (1995).

[27] O. Motrunich, S.-C. Mau, D. A. Huse, and D. S. Fisher, Phys. Rev. B **61**, 1160 (2000); Y.-C. Lin, N. Kawashima, F. Iglói, and H. Rieger, Prog. Theor. Phys. Suppl. **138**, 479 (2000); D. Karevski, Y-C. Lin, H. Rieger, N. Kawashima, and F. Iglói, Eur. Phys. J. B **20**, 267 (2001); Y-C. Lin, F. Iglói, and H. Rieger, Phys. Rev. Lett. **99**, 147202 (2007); R. Yu, H. Saleur, and S. Haas, Phys. Rev. B **77**, 140402 (2008).

[28] I. A. Kovács and F. Iglói, Phys. Rev. B **80**, 214416 (2009); **82**, 054437 (2010).

[29] I. A. Kovács and F. Iglói, Phys. Rev. B **83**, 174207 (2011); J. Phys.: Condens. Matter **23**, 404204 (2011).

[30] S. K. Ma, C. Dasgupta, and C.-K. Hu, Phys. Rev. Lett. **43**, 1434 (1979); C. Dasgupta and S. K. Ma, Phys. Rev. B **22**, 1305 (1980).

[31] For a review, see F. Iglói and C. Monthus, Phys. Rep. **412**, 277 (2005).

[32] A. P. Young and H. Rieger, Phys. Rev. B **53**, 8486 (1996).

[33] F. Iglói and H. Rieger, Phys. Rev. Lett. **78**, 2473 (1997); Phys. Rev. B **57**, 11404 (1998).

[34] C. Pich, A. P. Young, H. Rieger, and N. Kawashima, Phys. Rev. Lett. **81**, 5916 (1998).

[35] D. A. Matoz-Fernandez and F. Romá, arXiv:1512.03594.

[36] D. S. Fisher, Physica A **263**, 222 (1999).

[37] R. Juhász, I. A. Kovács, and F. Iglói, Europhys. Lett. **107**, 47008 (2014).

[38] C. Monthus, J. Stat. Mech. (2015) P05026; (2015) P10024.

[39] R. Juhász, J. Stat. Mech. (2014) P09027.

[40] R. Juhász, I. A. Kovács, and F. Iglói, Phys. Rev. E **91**, 032815 (2015).

[41] J. Galambos, *The Asymptotic Theory of Extreme Order Statistics* (Wiley, New York, 1978).

[42] E. Altman, Y. Kafri, A. Polkovnikov, and G. Refael, Phys. Rev. Lett. **93**, 150402 (2004); Phys. Rev. B **81**, 174528 (2010).

[43] R. B. Griffiths, Phys. Rev. Lett. **23**, 17 (1969); B. M. McCoy, *ibid.* **23**, 383 (1969).

[44] M. J. Thill and D. A. Huse, Physica A **214**, 321 (1995).

[45] P. W. Anderson and G. Yuval, Phys. Rev. Lett. **23**, 89 (1969).

[46] D. Thouless, Phys. Rev. **187**, 732 (1969).

[47] F. J. Dyson, Comm. Math. Phys. **21**, 269 (1971).

[48] J. L. Cardy, J. Phys. A **14**, 1407 (1981).

[49] M. Aizenman, J. Chayes, L. Chayes, and C. Newman, J. Stat. Phys. **50**, 1 (1988).

[50] J. Slurink and H. Hilhorst, Phys. A (Amsterdam, Neth.) **120**, 627 (1983).

[51] A. Bar and D. Mukamel, Phys. Rev. Lett. **112**, 015701 (2014).

[52] D. Poland and H. A. Scheraga, J. Chem. Phys. **45**, 1456 (1966).

[53] M. E. Fisher, J. Chem. Phys. **45**, 1469 (1966).

[54] R. Blossey and J. O. Indekeu, Phys. Rev. E **52**, 1223 (1995).

[55] M. E. Fisher, J. Stat. Phys. **34**, 667 (1984).

[56] D. J. Gross, I. Kanter, and H. Sompolinsky, Phys. Rev. Lett. **55**, 304 (1985).

[57] C. Toninelli, G. Biroli, and D. S. Fisher, Phys. Rev. Lett. **96**, 035702 (2006).

[58] C. Toninelli, G. Biroli, and D. S. Fisher, Phys. Rev. Lett. **98**, 129602 (2007).

[59] J. Schwarz, A. J. Liu, and L. Chayes, Europhys. Lett. **73**, 560 (2006).

[60] Y. Y. Liu, E. Csóka, H. Zhou, and M. Pósfai, Phys. Rev. Lett. **109**, 205703 (2012).

[61] W. Liu, B. Schmittmann, and R. Zia, Europhys. Lett. **100**, 66007 (2012).

[62] R. Zia, W. Liu, and B. Schmittmann, Phys. Procedia **34**, 124 (2012).

[63] L. Tian and D. N. Shi, Phys. Lett. A **376**, 286 (2012).

[64] G. Bizhani, M. Paczuski, and P. Grassberger, Phys. Rev. E **86**, 011128 (2012).

[65] M. Sheinman, A. Sharma, J. Alvarado, G. H. Koenderink, and F. C. MacKintosh, Phys. Rev. Lett. **114**, 098104 (2015).

[66] A. Bar and D. Mukamel, J. Stat. Mech. (2014) P11001.

[67] Y.-C. Lin, H. Rieger, N. Laflorencie, and F. Iglói, Phys. Rev. B **74**, 024427 (2006).

[68] J. Hooyberghs, F. Iglói, and C. Vanderzande, Phys. Rev. Lett. **90**, 100601 (2003); Phys. Rev. E **69**, 066140 (2004).

[69] T. Vojta and M. Dickison, Phys. Rev. E **72**, 036126 (2005).

[70] For the random LR contact process the discontinuity of the order parameter at the transition point is difficult to demonstrate numerically, at least for not too strong disorder. Here probably there is a disorder-dependent crossover, as has been seen in the SR model [68].